Journal of Hydrology 535 (2016) 270–281

Contents lists available at ScienceDirect

Journal of Hydrology

journal homepage: www.elsevier.com/locate/jhydrol

An explicit approach to capture diffusive effects in finite water-content method for solving vadose zone flow

Jianting Zhu [a,*], Fred L. Ogden [a], Wencong Lai [a,b], Xiangfeng Chen [a], Cary A. Talbot [c]

[a] Department of Civil and Architectural Engineering, University of Wyoming, Laramie, WY 82071, United States
[b] Currently at Clemson University, Clemson, SC 29634, United States
[c] Coastal and Hydraulics Laboratory, Engineer Research and Development Center, U.S. Army Corps of Engineers, Vicksburg, MS 39180, United States

ARTICLE INFO

Article history:
Received 22 September 2015
Received in revised form 28 January 2016
Accepted 30 January 2016
Available online 8 February 2016
This manuscript was handled by Corrado Corradini, Editor-in-Chief, with the assistance of Renduo Zhang, Associate Editor

Keywords:
Vadose zone flow
Finite water-content method
Water content bin
Diffusivity
Explicit method

SUMMARY

Vadose zone flow problems are usually solved from the Richards equation. Solution to the Richards equation is generally challenging because the hydraulic conductivity and diffusivity in the equation are strongly non-linear functions of water content. The finite water-content method was proposed as an alternative general solution method of the vadose zone flow problem for infiltration, falling slugs, and vadose zone response to water table dynamics based on discretizing the water content domain into numerous bins instead of the traditional spatial discretization. In this study, we develop an improved approach to the original finite water-content method (referred to as TO method hereinafter) that better simulates diffusive effects but retains the robustness of the TO method. The approach treats advection and diffusion separately and considers diffusion on a bin by bin basis. After discretizing into water content bins, we treat the conductivity and diffusivity in individual bins as water content dependent constant evaluated at given water content corresponding to each bin. For each bin, we can solve the flow equations analytically since the hydraulic conductivity and diffusivity can be treated as a constant. We then develop solutions for each bin to determine the diffusive water amounts at each time step. The water amount ahead of the convective front for each bin is redistributed among water content bins to account for diffusive effects. The application of developed solution is straightforward only involving algebraic manipulations at each time step. The method can mainly improve water content profiles, but has no significant difference for the total infiltration rate and cumulative infiltration compared to the TO method. Although the method separately deals with advection and diffusion, it can account for the coupling effects of advection and diffusion reasonably well.

1. Introduction

Quantifying flow of water through vadose zone soils is required for a large number of hydrological applications. Flow in unsaturated soils is often modeled using the Richards equation (RE) (Richards, 1931) and closed by hydraulic property functions to describe the relationship among pressures, saturations, and hydraulic conductivities (Caviedes-Voullieme et al., 2013; Liang and Uchida, 2014). The Richards equation is difficult to solve both analytically and numerically due to its parabolic form in combination with the strong non-linearity of the soil hydraulic functions (e.g., Brooks and Corey, 1964; van Genuchten, 1980; Vogel et al., 2001). Abrupt changes of water content in steep wetting fronts in dry soils, or drying fronts in wet soils, may pose challenging problems in numerical solutions of the Richards equation (Celia et al., 1990; Miller et al., 1998; van Dam and Feddes, 2000) in terms of the accuracy, stability, and rate of convergence of the numerical algorithms.

An alternative finite water-content method to the one-dimensional partial differential equation (PDE) for unsaturated porous media flow attributed to Richards (1931) was first proposed by Talbot and Ogden (2008). Recently a much improved and complete method was cast in a more rigorous physical and mathematical fashion (Ogden et al., 2015c). The finite water-content method (referred to as TO method hereinafter) is a general solution method of the vadose zone flow problem for infiltration, falling slugs, and vadose zone response to water table dynamics in an unsaturated porous medium (e.g., Ogden et al., 2015b). The method represents a significant advance to overcome many issues related to numerically solving the Richards equation in that it can simulate sharp fronts, and is guaranteed to converge using a finite-volume

* Corresponding author. Tel.: +1 307 766 4375; fax: +1 307 766 2221.
E-mail address: jzhu5@uwyo.edu (J. Zhu).

http://dx.doi.org/10.1016/j.jhydrol.2016.01.078
0022-1694/

solution. The method can be easily incorporated in simulations of large watersheds or in regional climate-hydrology models where solving the RE at millions of nodes is required without the risk of non-convergence often encountered in the numerical solutions of the Richards equation, which often jeopardizes the stability of the entire model simulation (Ogden et al., 2015c). The fact that the finite water content method is arithmetic and an explicit solution of ordinary differential equation suggests that it will be amenable to significant improvements in computational efficiency. Therefore, the method is particularly useful in applications such as high-resolution quasi-3D simulations of large-scale climate and hydrology problems (Ogden et al., 2015a).

A distinguishing characteristic of the TO method is the discretization of the water content domain into "bins" of water content $\Delta\theta$, leaving the vertical spatial dimension as a continuum over which the model can freely move wetting and drying fronts. The TO method is advective, driven by gravity and capillary gradients, and without an explicit representation of soil water diffusivity (Ogden et al., 2015c). This is similar to the idea behind the Green–Ampt equation (Green and Ampt, 1911), but it is considered for each individual water content bin.

The main objective of this study is to incorporate soil water diffusivity into the TO method to improve water content profiles. A key concept in the proposed method is to consider diffusive effects on the basis of individual water content bins. Three new ideas are integrated in the analytical developments as described below. First, we solve water content advection–diffusion equation to develop water content profile for each bin. The velocity term in the equation is similar to the TO method. Since the water content domain is discretized into numerous bins, the diffusivity for the bin is approximated as a constant evaluated at the water content for that bin and the wetting front moving velocity is calculated for each time step based on the TO method. Second, we determine the total amount of water that is ahead of the advective wetting front due to diffusive effects. This amount of water is determined by integrating water content ahead of wetting front at each time step, which can be performed analytically. Finally, the water amount due to the diffusive effects is re-distributed among bins to simulate the effects of diffusion on the water content profiles.

Based on the above concepts, the developed solution in this study only involves algebraic calculations with no need to solve differential equations in determining the diffusive effects. The advective portion of the solutions is determined by solving a simple ordinary differential equation similar to the TO method. Since both diffusivity and hydraulic conductivity are a strong nonlinear function of water content, they are bin-dependent (i.e., water content dependent) which is the main reason that the Richards equation is difficult to solve numerically, especially in advection dominated problems. Our method separates advective and diffusive effects for each individual water content bin. We then evaluate the developed solution for problems related to two extreme ends of advection and diffusion by comparing the results in this study to those from numerical solutions of the Richards equation.

2. Methods

Since the main objective of this study is to incorporate soil water diffusivity into the TO method, we first briefly recapture the main ideas of the TO method (Talbot and Ogden, 2008; Ogden et al., 2015c). Please refer to Ogden et al. (2015c) for more details. The TO method is an approximate general solution method of one-dimensional unsaturated zone flow problem for infiltration, falling slugs, and vadose zone response to water table dynamics that includes gravity and capillary gradients, but neglects soil water diffusivity. The main concept is represented in Fig. 1, which illustrates that the porous medium is divided into N discrete segments of water content space called "bins", $\Delta\theta$, between the residual water content θ_r and saturated water content, θ_s. The TO method mainly deals with three processes. The first process is the infiltration front, as shown in green in Fig. 1. The second is the falling slug as shown in purple in Fig. 1. The third is the water held up by capillarity that is in contact with a groundwater table as shown in blue in Fig. 1. In this study, our focus is on the infiltration front.

Water advances through a front that spans water content ranging from the wettest (right most) bin with the water content θ_0 to driest (left most) bin with the water content of θ_{ini} in the water content profile. The TO method is built on the same principles in deriving the Richards equation but uses the cyclic chain rule to determine how each water content bin moves in the z direction (Fig. 1) over time. The following equation of determining how wetting front z in representing the water content bin θ can be then derived,

$$\left(\frac{dz}{dt}\right)_\theta = \frac{\partial K(\theta)}{\partial\theta}\left(1-\frac{\partial\psi(\theta)}{\partial z}\right) - \frac{K(\theta)}{(\partial\theta/\partial z)}\frac{\partial^2\psi(\theta)}{\partial z^2} \quad (1)$$

where $K(\theta)$ is the hydraulic conductivity at water content θ, and ψ is the capillary pressure head. The fundamental assumption of the TO method is that the infiltration wetting front ψ is single valued everywhere along the wetting front. Ogden et al. (2015c) demonstrated that the second term in the right-hand side of Eq. (1) is small, which may be neglected. We then have the following equation,

$$\left(\frac{dz}{dt}\right)_\theta = \frac{\partial K(\theta)}{\partial\theta}\left(1-\frac{\partial\psi(\theta)}{\partial z}\right) \quad (2)$$

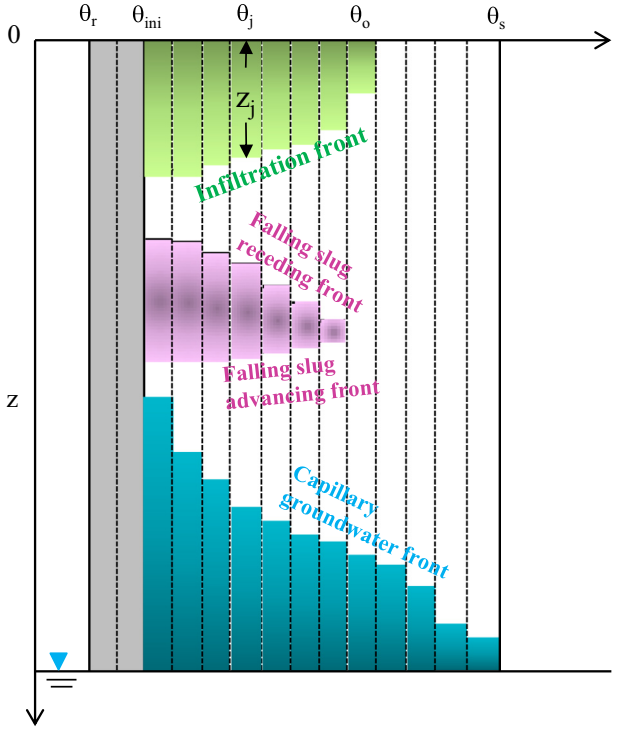

Fig. 1. Discretization in water content domain and three water content profile fronts as conceptualized in Ogden et al. (2015c) including infiltration fronts (top, green), falling slugs (middle, purple), and capillary groundwater fronts (bottom, blue) (modified based on Ogden et al. (2015c)). In this study, we mainly seek to improve infiltration fronts, where z_j varies with both water content bin θ_j and time t_i. (For interpretation of the references to color in this figure legend, the reader is referred to the web version of this article.)

In the case of infiltration front, the resulting equation to determine the front location of water content bin j is as follows (Ogden et al., 2015c),

$$\frac{dz_j}{dt} = \frac{K(\theta_0) - K(\theta_{ini})}{\theta_0 - \theta_{ini}}\left(1 + \frac{G_{eff} + h_p}{z_j}\right) \quad (3)$$

where z_j is the depth of water content bin j, G_{eff} has the same value for all bins, which is an integral metric for representing the impact of capillarity ahead of wetting front and h_p is the depth of ponded water on the surface in the case of infiltration. The wetting front effective capillary drive G_{eff} is the greater of $|\psi(\theta_0)|$ or the value calculated as described by Morel-Seytoux et al. (1996). The depth of water content bin j at time step i based on the TO method, $z_{j,i(TO)}$ can be determined by solving the simple ordinary Eq. (3).

For the situations when the surface has constant ponded depth (i.e., h_p = constant in the above equation) at all time, this equation will produce a sharp wetting front since evolution of z_j with time is the same for every water content bin. In this paper, we propose an approach (called TO Diffusion hereinafter) built on the idea of discretization over water content domain to incorporate diffusive effects into the solution.

For each bin where the diffusivity can be approximated as a constant evaluated at the water content at this water content bin, we use a linearized equation of advection and diffusion (Ogata and Banks, 1961; Menziani et al., 2007),

$$\frac{\partial\theta}{\partial t} = D\frac{\partial^2\theta}{\partial z^2} - U\frac{\partial\theta}{\partial z} \quad (4)$$

where D is the diffusivity evaluated at water content for each individual bin, and $U = dz/dt$ is the wetting front moving velocity calculated from the TO method. The initial condition is $\theta(z,0) = \theta_{ini}$. Note that the boundary conditions are the same for all bins which extend from the surface to the wetting front, $\theta(0,t) = \theta_0$; $\theta(\infty,t) = \theta_{ini}$ (see Fig. 2). The solution to the above equation can be obtained (e.g., Ogata and Banks, 1961):

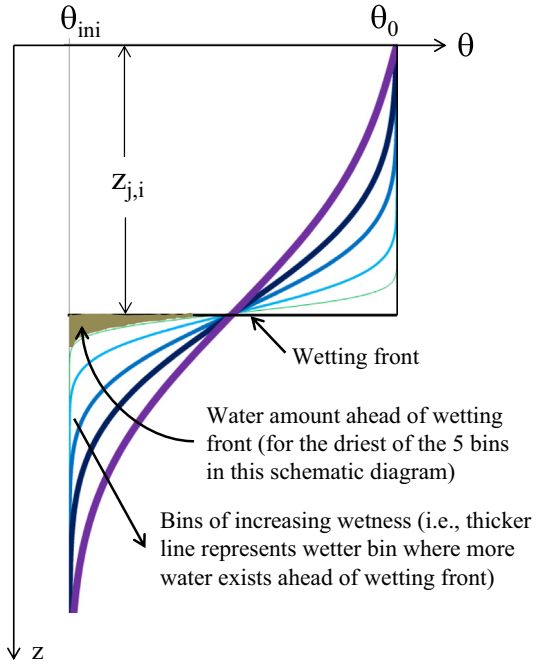

Fig. 2. Water content profiles in various water content bins calculated based on Eq. (5). In developing these profiles, wetting front location $z_{j,i}$ and velocity $U_{j,i}$ for each time step are calculated from the finite water-content method (TO method) and soil diffusivity D_j for each bin is calculated based on the water content at that bin.

$$\Theta(z,t) = \frac{\theta(z,t) - \theta_{ini}}{\theta_0 - \theta_{ini}} = \left(\frac{1}{2}\right)\left\{\mathrm{erfc}\left[\frac{z-Ut}{2\sqrt{Dt}}\right] + \exp\left(\frac{Uz}{D}\right)\mathrm{erfc}\left[\frac{z+Ut}{2\sqrt{Dt}}\right]\right\} \quad (5)$$

The requirement for this solution is that both D and U are constant, which is reasonable for each individual bin. But D and U will vary between bins. We then determine the diffusive effects by calculating the water amount ahead of the advective front (i.e., $z_{j,i}$) (Fig. 2) for each time step based on the above equation. Therefore, we also assume that the wetting front velocity U_j, does not change significantly within one time step. The difference of water amount ahead of the advective front between two consecutive time steps is re-distributed among bins to account for the diffusive effects.

The key assumption here is that we separate the advective and diffusive processes at each time step. The advective wetting front is treated by the TO method in Eq. (3) above, and the diffusive effects are dealt with using the method presented below. The diffusivity varies among the bins. The velocity U_j also varies among the bins and also at different time steps. As a result, the solutions also vary among the bins. The water content profiles with larger spreading represent wetter bins. The main mechanism is due to larger diffusivity for the wetter bin associated with higher water content.

The water amount ahead of the wetting front (one example is shown as the shaded area for the driest bin depicted in Fig. 2) can be calculated by the following integration,

$$W = \int_{Ut}^{\infty}(\theta(z,t) - \theta_{ini})dz \quad (6)$$

Note that the integration in Eq. (6) is from Ut to ∞, which represents the total net amount of water due to infiltration ahead of the wetting front located at Ut. The above integration is performed for all water content bins, and its value is larger for the wetter bins. Using θ from Eq. (5), we have,

$$W = \left(\frac{1}{2}\right)(\theta_0 - \theta_{ini})\int_{Ut}^{\infty}\left\{\mathrm{erfc}\left[\frac{z-Ut}{2\sqrt{Dt}}\right] + \exp\left(\frac{Uz}{D}\right)\mathrm{erfc}\left[\frac{z+Ut}{2\sqrt{Dt}}\right]\right\}dz \quad (7)$$

The integration can be performed analytically to get (see Appendix),

$$W = \left(\sqrt{\frac{Dt}{\pi}}\right)(\theta_0 - \theta_{ini})\left\{1 + \frac{\sqrt{\pi}[1 - \exp(\xi^2)\mathrm{erfc}(\xi)]}{2\xi}\right\} \quad (8)$$

At two time steps between t_i (=$t + \Delta t$) and t_{i-1} (=t), the difference between $W|_{t_i}$ and $W|_{t_{i-1}}$ is the diffusive amount of water requiring redistribution among bins,

$$\Delta W = W|_{t_i} - W|_{t_{i-1}} \quad (9)$$

with

$$W|_{t_i} = \left(\sqrt{\frac{Dt_i}{\pi}}\right)(\theta_0 - \theta_{ini})\left\{1 + \frac{\sqrt{\pi}[1 - \exp(\xi_{t_i}^2)\mathrm{erfc}(\xi_{t_i})]}{2\xi_{t_i}}\right\} \quad (10)$$

$$W|_{t_{i-1}} = \left(\sqrt{\frac{Dt_{i-1}}{\pi}}\right)(\theta_0 - \theta_{ini})\left\{1 + \frac{\sqrt{\pi}\left[1 - \exp(\xi_{t_{i-1}}^2)\mathrm{erfc}(\xi_{t_{i-1}})\right]}{2\xi_{t_{i-1}}}\right\} \quad (11)$$

where

$$\xi_{t_i} = \frac{Ut_i}{\sqrt{Dt_i}} \quad (12)$$

$$\xi_{t_{i-1}} = \frac{Ut_{i-1}}{\sqrt{Dt_{i-1}}} \quad (13)$$

The diffusive distance is related to water amount by,

$$\Delta z = \Delta W/(\theta_0 - \theta_{\text{ini}}) \tag{14}$$

In Eq. (14), the total amount divided by the initial water deficit represents the actual diffusive distance in the domain. The diffusive distance for redistribution for the water content bin j at time step i is then,

$$\Delta z_{j,i} = \frac{1}{2}\sqrt{\frac{D_j}{\pi}}\left\{\sqrt{t_i} - \sqrt{t_{i-1}} + \left[\frac{\sqrt{\pi}(1-\exp(\xi_{j,i}^2)\text{erfc}(\xi_{j,i}))}{2\xi_{j,i}}\right]\sqrt{t_i} - \left[\frac{\sqrt{\pi}(1-\exp(\xi_{j,i-1}^2)\text{erfc}(\xi_{j,i-1}))}{2\xi_{j,i-1}}\right]\sqrt{t_{i-1}}\right\} \tag{15}$$

where

$$\xi_{j,i} = \frac{U_{j,i}t_i}{\sqrt{D_j t_i}} \tag{16}$$

$$\xi_{j,i-1} = \frac{U_{j,i-1}t_{i-1}}{\sqrt{D_j t_{i-1}}} \tag{17}$$

This diffusive distance for each bin j at any time step t_i is redistributed according to the scheme shown in Fig. 3. Fig. 3(a) schematically illustrates the water profile results from the TO method, where $z_{j,i(\text{TO})}$ is the water content profile calculated by the TO Eq. (3) for the water content bin j at time step i. Fig. 3(b) illustrates the diffusive distance ahead of the advective wetting front, $\Delta z_{j,i}$ calculated based on Eq. (15) for bin j at time step i. We calculate the average diffusive distance based on the shaded area in Fig. 3(b), $\overline{\Delta z_i} = \frac{1}{N}\sum_{j=1}^{N}\Delta z_{j,i}$. Then we redistribute the diffusive distance for each bin (i.e., Fig. 3(b)) to the profile in Fig. 3(a) by keeping the total water amount the same as that from Fig. 3 (a). The water content shown in Fig. 3(d) (i.e., Fig. 3(c) minus the shaded portion) represents the profile with diffusive effects at time t_i, $z_{j,i}$. We can then move to the next time step and repeat the same procedure.

3. Benchmarking process

To evaluate and discuss the effectiveness of the TO Diffusion, we will compare the results from the developed TO Diffusion method with those from the finite volume predictor–corrector (FVPC) method with adaptive time-stepping to solve the one-dimensional Richards equation (Lai and Ogden, 2015) for 11 common soil textural classifications shown in Fig. 4 from Rawls et al. (1982, 1983). The FVPC method with adaptive time-stepping was developed to solve the one-dimensional Richards equation by Lai and Ogden (2015) to overcome mass balance errors and numerical oscillation and dispersion. The FVPC is mass-conservative and non-iterative. In the predictor step, the pressure head is updated by solving the pressure head-based Richards equation using the cell-centered finite volume method with a semi-implicit temporal scheme. In the corrector step, the soil water content is calculated using the mixed form Richards equation with an explicit scheme.

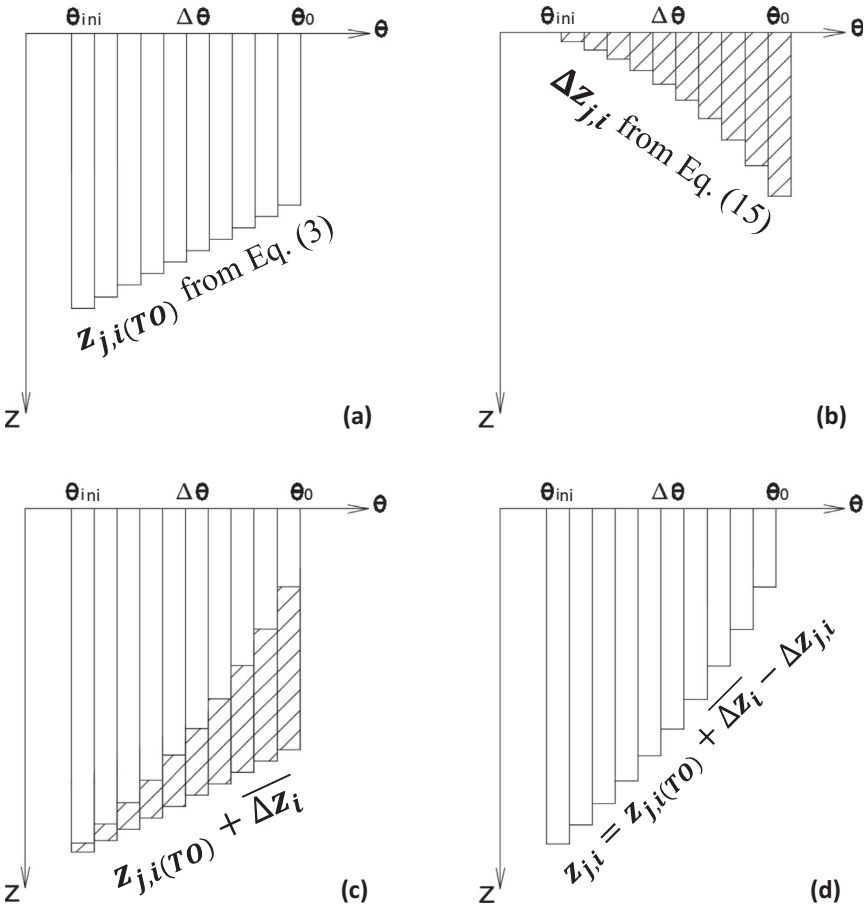

Fig. 3. Schematic illustration of the proposed water content re-distribution to account for diffusive effects. (a) At time step i, advancing distance for bin j calculated from the TO method Eq. (3), (b) diffusive depth $\Delta z_{j,i}$ is obtained from Eq. (15), (c) $\overline{\Delta z_i}$ calculated as the average depth from (b) is added to each water content bin in (a), (d) final water content profile at time step i. The re-distribution steps in (c) and (d) are to make sure that the profile shown in (d) has the same total amount of water as that in (a) after the diffusive depth $\Delta z_{j,i}$ is re-distributed.

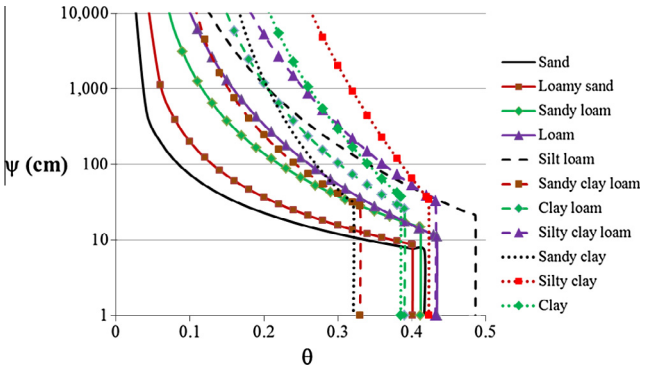

Fig. 4. Soil water retention curves based on the Brooks–Corey (1964) hydraulic property model for the 11 texture classifications. The hydraulic parameters for the Brooks–Corey model are from Rawls et al. (1982, 1983).

Explicit treatment for cells at the saturated–unsaturated interface is also specifically given. The performance of the FVPC scheme has been evaluated in simulating infiltration into wet and dry soils, infiltration with a falling water table, and free drainage by comparing with measurements, HYDRUS-1D (Simunek et al., 2009), or analytical solutions when available. The comparison results demonstrated that the FVPC scheme is robust, mass conservative and accurate in simulating variably saturated flows with various boundary conditions.

We will consider infiltration processes when the inlet surface is kept saturated. Both horizontal and vertical infiltrations are considered, which represent two extreme ends of diffusion and advection scenarios to evaluate the developed method in this study. The diffusive effects are more pronounced in horizontal infiltration than in vertical infiltration. Under these conditions, the TO method would simulate sharp (piston-type) water content profiles without

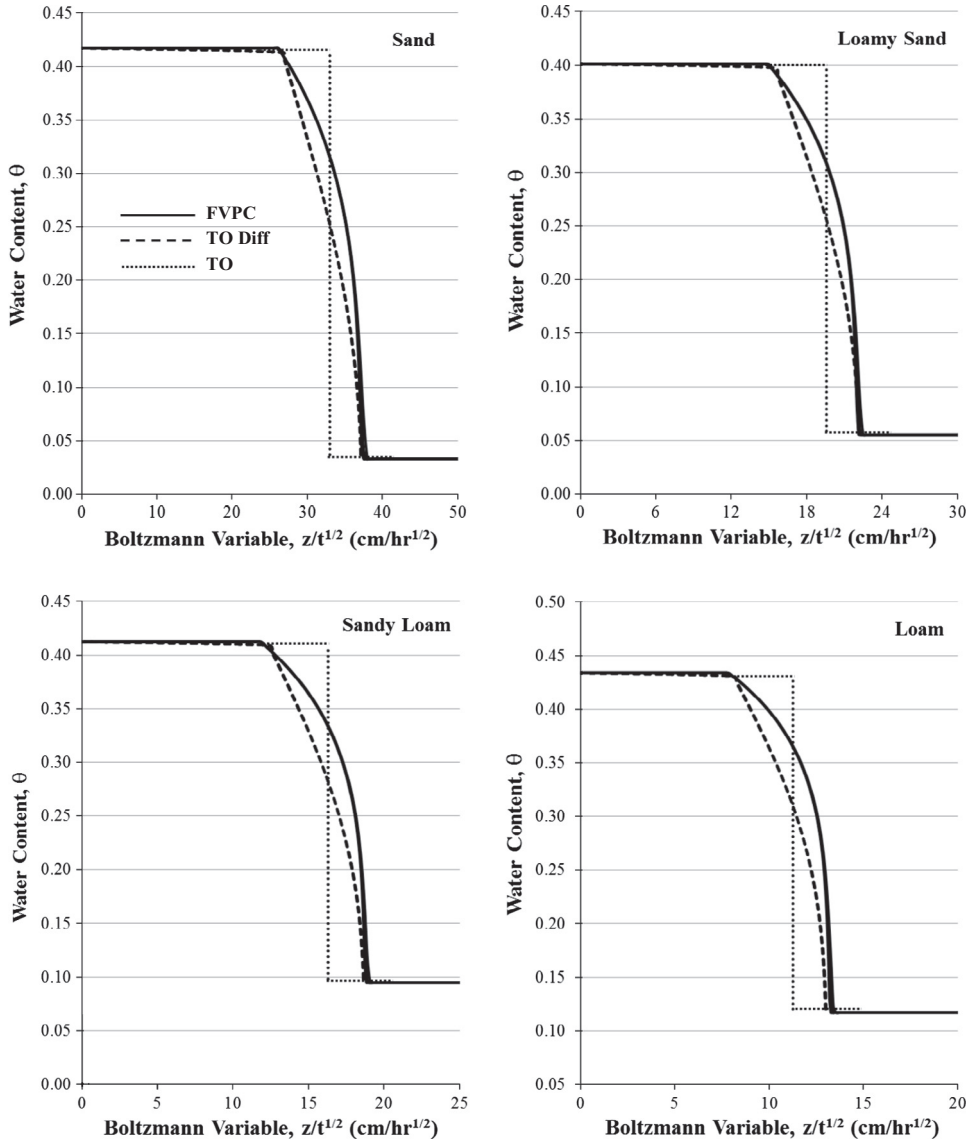

Fig. 5. Comparison of horizontal infiltration water content profiles from FVPC, TO, and TO Diffusion methods for sand, loamy sand, sandy loam and loam. Note that for each method there are three times in each plot. Due to the Boltzmann scaling in horizontal infiltration, results for the 3 times reduce to almost a single curve, which demonstrate that all three methods conform to the Boltzmann scaling well. The three times are respectively: 0.25, 0.5, 1.0 h for sand; 1, 2, 4 h for loamy sand; 2, 4, 8 h for sandy loam; and 3, 6, 12 h for loam.

diffusion, similar to the one from the Green–Ampt method (Green and Ampt, 1911).

For the horizontal infiltration, if we adopt Boltzmann variable $= \frac{z}{\sqrt{t}}$, then the Richards equation

$$\frac{\partial\theta}{\partial t} = \frac{\partial}{\partial z}\left[D(\theta)\frac{\partial\theta}{\partial z}\right] \tag{18}$$

can be transformed into an ordinary equation in terms of ϕ

$$\frac{-\phi}{2}\frac{d\theta}{d\phi} = \frac{d}{d\phi}\left[D(\theta)\frac{d\theta}{d\phi}\right] \tag{19}$$

Since Eq. (19) is an ordinary differential equation, it demonstrates that the water content is only a function of the Boltzmann variable ϕ for the horizontal infiltration. Therefore, this resulting equation enables us to scale water content profiles at different times into one single profile. The comparison of water content profiles can then be made in terms of the Boltzmann variable ϕ without the need to compare at different times. Note that generally water content is a function of both z and t. By combining z and t into the Boltzmann variable, the water content is only related to ϕ. This is only possible for horizontal infiltration. Therefore, we can plot water content profiles at different times in terms of ϕ for horizontal infiltration to check whether artificial numerical diffusion exists in any solutions.

The soil hydraulic properties are required to describe the water content $\theta(\psi)$, unsaturated hydraulic conductivity $K(\theta)$ and diffusivity $D(\theta)$. In illustrating the method, we use the Brooks–Corey model (Brooks and Corey, 1964) to represent soil hydraulic properties. However, any other hydraulic property models can also be used easily.

$$\frac{\theta-\theta_r}{\theta_s-\theta_r} = \left(\frac{\psi}{\psi_b}\right)^{-\lambda} \quad \psi > \psi_b \tag{20a}$$

$$\theta = \theta_s \quad \psi \leqslant \psi_b \tag{20b}$$

$$K(\theta) = K_s\left(\frac{\theta-\theta_r}{\theta_s-\theta_r}\right)^{(\ell+2)+\frac{2}{\lambda}} \quad \theta < \theta_s \tag{21a}$$

$$K(\theta) = K_s \quad \theta = \theta_s \tag{21b}$$

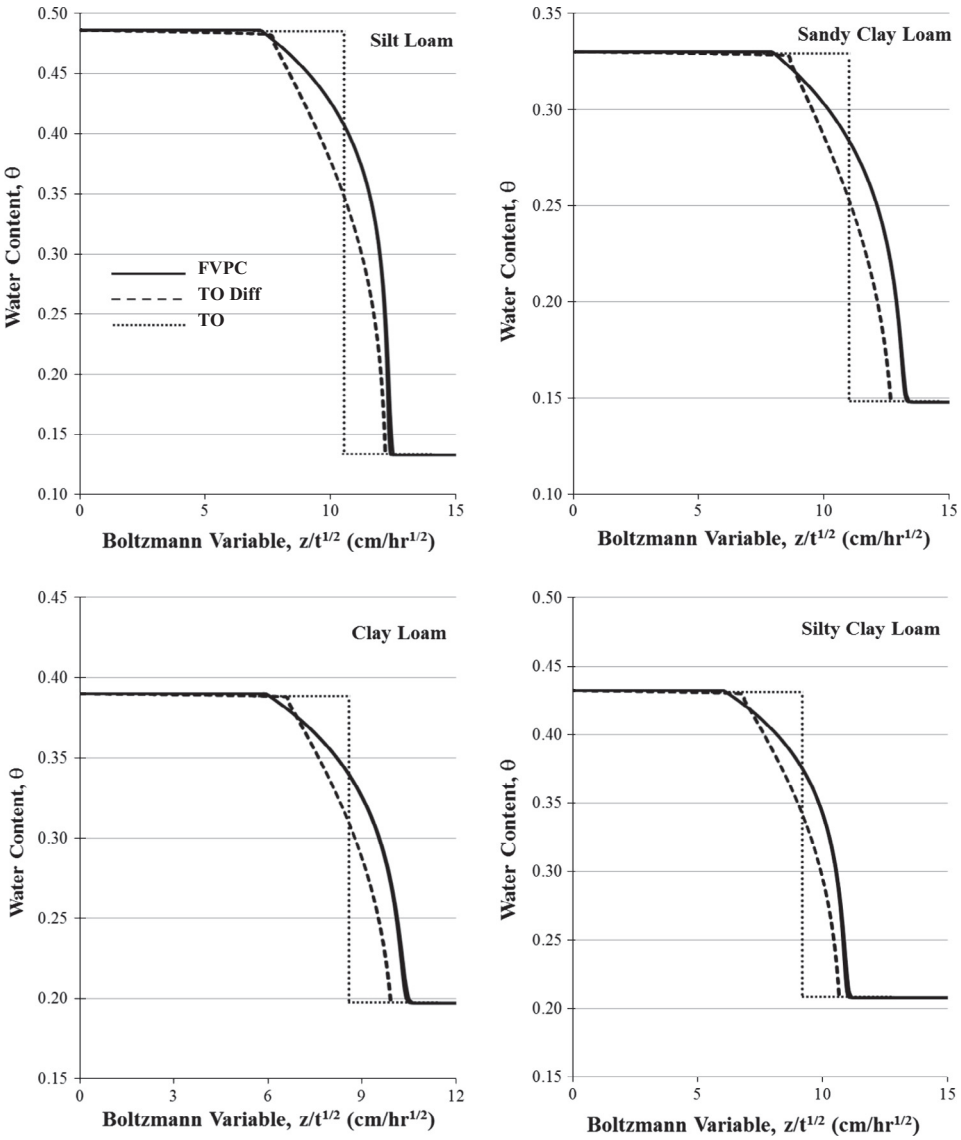

Fig. 6. Comparison of horizontal infiltration water content profiles from FVPC, TO, and TO Diffusion methods for silt loam, sandy clay loam, clay loam and silty clay loam. Note that for each method there are three almost identical curves each plot representing three times. The three times are respectively: 5, 10, 15 h for silt loam; 5, 10, 15 h for sandy clay loam; 5, 10, 20 h for clay loam; and 5, 10, 20 h for silty clay loam.

The soil diffusivity can be expressed as,

$$D(\theta) = K(\theta)\frac{\partial\psi(\theta)}{\partial\theta} \tag{22}$$

$$D(\theta) = \frac{\psi_b K_s}{\lambda(\theta_s-\theta_r)}\left(\frac{\theta-\theta_r}{\theta_s-\theta_r}\right)^{(\ell+1)+\frac{1}{\lambda}} \quad \theta < \theta_s \tag{23a}$$

$$D(\theta) = \infty \quad \theta = \theta_s \tag{23b}$$

where θ_s and θ_r are the saturated and residual water contents respectively, ψ_b is the bubbling pressure head, λ is the dimensionless pore-size distribution parameter, K_s is the saturated hydraulic conductivity, and ℓ is a parameter to account for the dependence of the tortuosity and the correlation factors on the water content. In this study, we use $\ell = 1$.

Based on the hydraulic conductivity function above, the effective capillary drive can be integrated as,

$$G_{\text{eff}} = \frac{1}{K_s}\int_0^{\infty} K(\psi)d\psi = \frac{1}{K_s}\int_0^{\psi_b} K_s d\psi + \frac{1}{K_s}\int_{\psi_b}^{\infty} K(\psi)d\psi$$
$$= \psi_b\left[\frac{\lambda(\ell+2)+1+1}{\lambda(\ell+2)+1}\right] = \psi_b\left[\frac{\lambda(\ell+2)+2}{\lambda(\ell+2)+1}\right] = \psi_b\left(\frac{3\lambda+2}{3\lambda+1}\right) \tag{24}$$

The comparison with the FVPC results is presented for 11 common soil textural classifications of Rawls et al. (1982, 1983) for the surface θ at saturated water content (i.e., $\theta_0 = \theta_s$) at all times $t > 0$. It is assumed that each soil was well drained with an initial volumetric water content, θ_{ini}, equal to the wilting point water content.

4. Results and discussion

In Figs. 5–7, we show the comparison of simulation results of water content profiles for all 11 soil classes for the horizontal infiltration. In calculating these results by the TO Diffusion method, we discretized the water content domain into 200 bins and used a time step ranging from 0.005 h. for sand to 0.2 h. for clay. The water content profile results from all three methods (i.e., TO, TO Diffusion, and FVPC), conform to the Boltzmann scaling well. This can be seen from the fact that water content profiles at different times all reduce into a single profile if they are plotted using the Boltzmann variable. In general, the TO Diffusion approach can improve the water content profiles but still under-estimates the diffusive effects. The main reason may be due to the fact that diffusive effects are most pronounced for horizontal infiltration. The

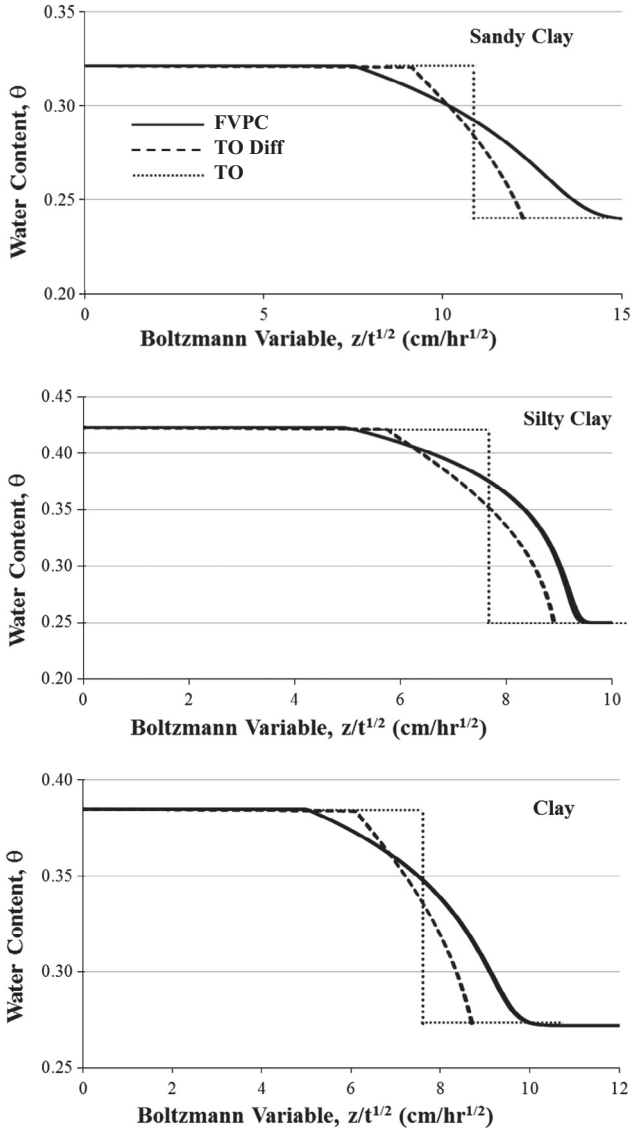

Fig. 7. Comparison of horizontal infiltration water content profiles from FVPC, TO, and TO Diffusion methods for sandy clay, silty clay, and clay. Note that for each method there are three almost identical curves each plot representing three times. The three times are respectively: 5, 10, 15 h for sandy clay; 5, 10, 20 h for silty clay; and 5, 20, 40 h for clay.

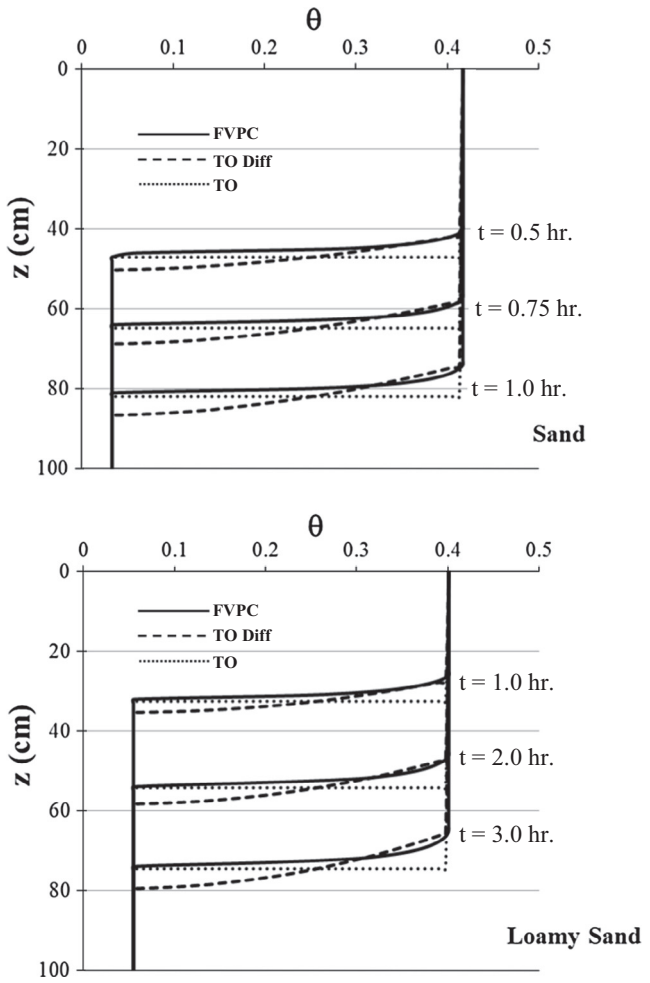

Fig. 8. Vertical infiltration water content profiles from FVPC, TO, and TO Diffusion methods at three selected times for sand and loamy sand.

only advective effect is due to the integral metric of capillarity ahead of wetting front from dry soil ahead of the wetting front. On the other hand, capillarity also facilitates diffusive effects by promoting water content gradient. Therefore, these two effects are coupled. While the TO Diffusion approach to separately deal with these two effects can improve water content profiles, it is still difficult to fully account for the coupling effects of advection and diffusion.

The results of water content profiles in vertical infiltration are shown in Figs. 8–11. The water content domain discretization and time step used were the same as the horizontal infiltration cases for the TO Diffusion method. Contrary to the horizontal infiltration cases, the TO Diffusion method over-estimates diffusive effects for coarse textural classes (sand and loam classes), which can be observed from Figs. 8–10. However, the TO Diffusion approach under-estimates diffusive effects for the fine textural classes (clay classes), which are observable from Fig. 11. For coarse texture classes, the main mechanism in vertical infiltration is highly advective and fast moving due to the combined effects of gravity and high hydraulic conductivity. In these cases, the TO Diffusion method introduces pronounced diffusive effects for coarse texture soils.

By separating diffusion from advection in this study, we can analyze quantitatively how the diffusive effects evolve when flow scenario changes from horizontal infiltration to vertical infiltration. Most pronounced diffusive effects exist when $U \approx 0$ which means the process is highly diffusive. It can be shown that when flow scenario switches from $U \to 0$ to $U \to \infty$, the diffusive effects decrease by a factor of two (see Appendix),

$$\frac{\lim_{\xi_t \to 0} \Delta W}{\lim_{\xi_t \to \infty} \Delta W} = 2 \tag{25}$$

Therefore, the largest difference is two times in the diffusive amount that needs to be re-distributed among the water content bins when we try to separate advection and diffusion by the TO

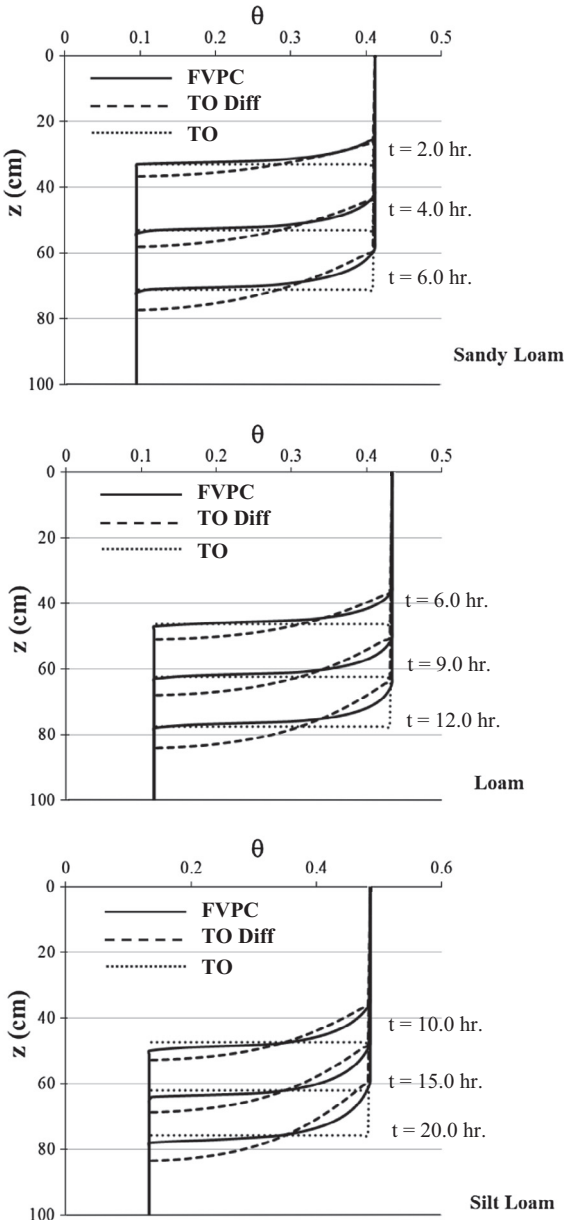

Fig. 9. Vertical infiltration water content profiles from FVPC, TO, and TO Diffusion methods at three selected times for sandy loam, loam, and silt loam.

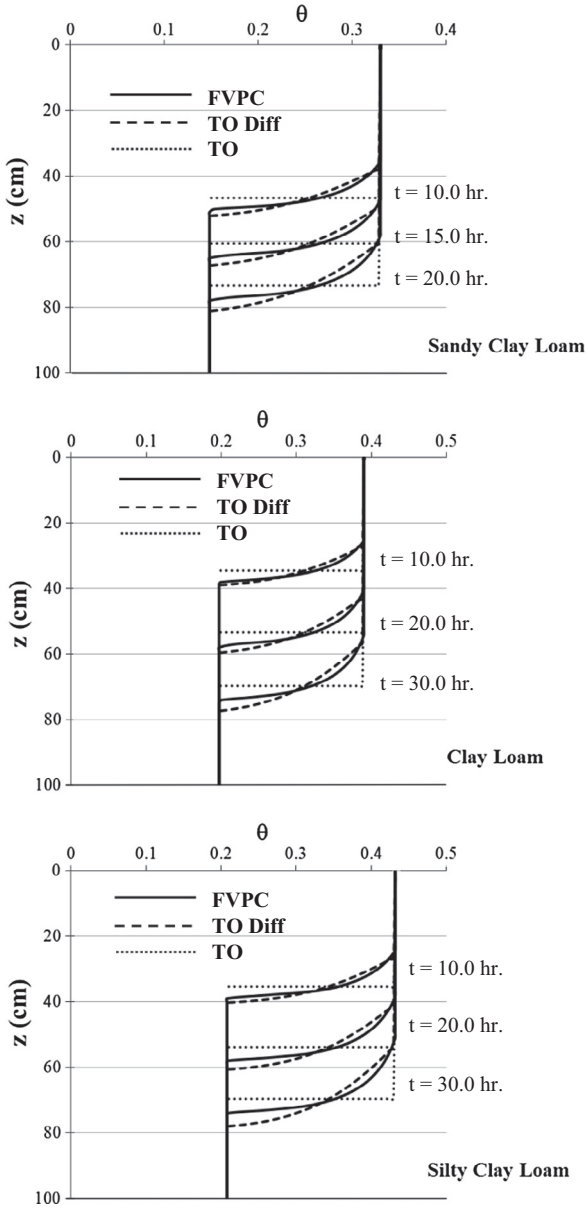

Fig. 10. Vertical infiltration water content profiles from FVPC, TO, and TO Diffusion methods at three selected times for sandy clay loam, clay loam, and silty clay loam.

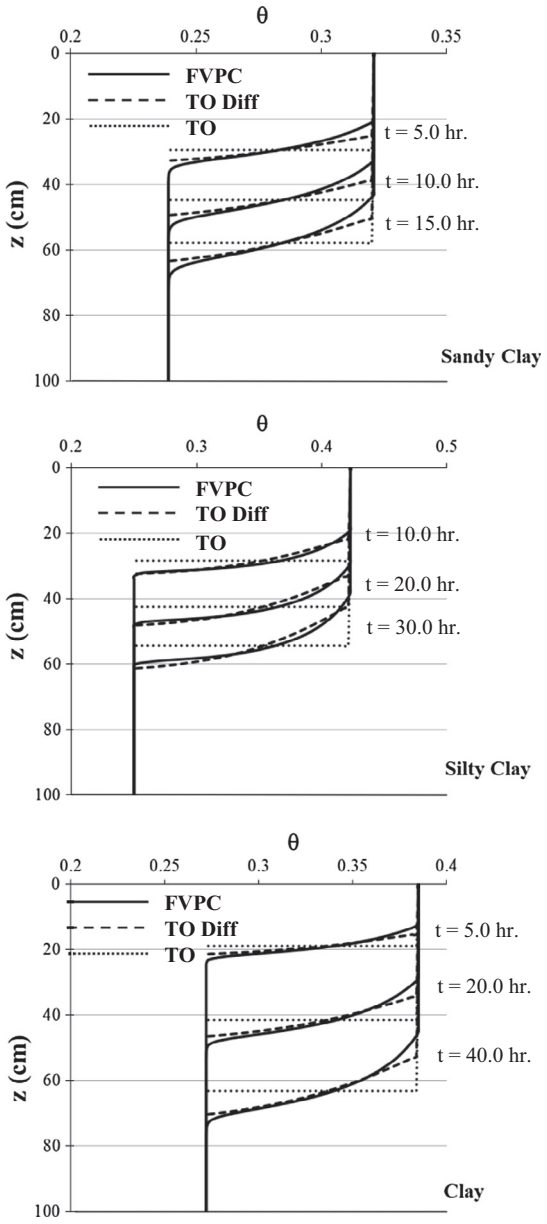

Fig. 11. Vertical infiltration water content profiles from FVPC, TO, and TO Diffusion methods at three selected times for sandy clay, silty clay, and clay.

Diffusion method. While it can improve diffusive effects in general, this maximum difference by a factor of 2 may not be enough to cover the full spectrum from advection dominated to diffusion dominated processes. For vertical infiltration in coarse textural soils, fast advection due to gravity and capillarity may suppress diffusive effects to a higher degree of more than 2 times. This signifies the fact that diffusive and advective effects are inherently coupled and advection may suppress diffusive effects. The coupling effects are under-estimated by the TO Diffusion method developed in this study.

In Table 1, we summarize the root mean square errors (RMSEs) for all cases presented in Figs. 5–11 for a quantitative comparison. For the horizontal infiltration, the RMSEs are in terms of the Boltzmann variable, while for the vertical infiltration the RMSEs are in terms of the actual infiltration depth. We can see that the TO Diffusion method produces much improved water content profile results for all 11 textural classes for the horizontal infiltration cases, which can be seen from the smaller RMSEs than the TO method as listed in Table 1. For the vertical infiltration, however, the TO Diffusion generates larger RMSEs than the TO for coarse textural classes due to the more pronounced water content profile spreading compared with the FVPC method. For medium and fine textural classes, the TO Diffusion method produces better water content profiles than the TO method. Table 2 explicitly lists the percent changes of RMSE between the TO Diffusion and the TO methods for the scenarios examined in this study, where negative percent changes mean better agreement with the results from the FVPC simulations. With the exception of vertical infiltration for the coarse textural soils, the TO Diffusion approach produces better water content profiles for all the other cases. The results demonstrate that the percent changes of RMSE between TO Diffusion and TO methods range from −78% to +36% with an overall average percent change of −34% for vertical infiltration. For horizontal infiltration, the percent changes of RMSE range from −40% to −62% with an average of −54%, which indicates that the proposed TO Diffusion method works better for all the cases of horizontal infiltration we examined. Overall, the TO Diffusion reduces the RMSE by 39% if we consider both vertical and horizontal infiltrations, which means that the proposed TO Diffusion approach can better simulate water content profiles than the TO method. However, the proposed method over-simulate diffusive effects for the coarse soil types (sand, loamy sand, sandy loam, and loam) signified by the increased RMSE ranging from 4.5% to 36% with an average increase in RMSE of 7.5% for those 4 types of soil.

It is also worthwhile to note that while the TO Diffusion method generally improves diffusive effects and water content profiles, the

Table 1
Root mean square errors (RMSEs) of the water content profile variables for the TO Diffusion and TO methods when compared to the finite volume predictor–corrector (FVPC) Richards equation solver. Note that the water content profile variable for comparison is the Boltzmann variable for the horizontal infiltration and infiltration depth for the vertical infiltration.

Texture	Horizontal (cm/h$^{1/2}$)		Vertical (cm)					
			t_1		t_2		t_3	
	TO Diff	TO	TO Diff	TO	TO Diff	TO	TO Diff	TO
Sand	1.6	3.8	1.2	1.5	2.5	2.3	2.8	2.5
Loamy sand	0.8	2.2	1.6	2.2	2.9	2.7	3.6	3.0
Sandy loam	0.9	2.0	2.4	2.6	3.2	3.1	3.8	3.5
Loam	0.8	1.6	3.0	2.7	3.8	3.0	4.5	3.3
Silt loam	0.7	1.5	2.5	3.4	3.2	4.0	4.0	4.4
Sandy clay loam	0.8	1.6	1.1	3.3	1.7	3.7	2.2	4.1
Clay loam	0.6	1.4	0.8	3.7	1.5	4.6	2.0	5.3
Silty clay loam	0.6	1.4	1.1	3.4	1.8	4.5	2.4	5.3
Sandy clay	1.4	2.4	1.5	3.8	2.2	5.2	2.3	6.1
Silty clay	0.5	1.3	0.8	3.5	1.0	4.6	1.4	5.5
Clay	0.7	1.4	1.0	2.9	1.7	5.3	2.0	7.1

Table 2
Percent change in the root mean square error (RMSE[a]) between the TO Diffusion and TO methods when they are compared with the finite volume predictor–corrector (FVPC) Richards equation solver for both horizontal and vertical infiltrations.

	Vertical						Horizontal
	Time when profiles were calculated in vertical			Percent change in RMSE[b]			
Texture	t_1 (h)	t_2 (h)	t_3 (h)	t_1	t_2	t_3	
Sand	0.25	0.50	1.00	−15.1	7.2	14.5	−57.0
Loamy sand	1.00	2.00	4.00	−26.4	7.4	20.2	−61.4
Sandy loam	2.00	4.00	8.00	−8.2	4.5	10.5	−55.2
Loam	3.00	6.00	12.00	14.1	24.7	36.2	−47.0
Silt loam	5.00	10.00	15.00	−26.0	−19.8	−10.1	−51.2
Sandy clay loam	5.00	10.00	15.00	−65.6	−53.7	−45.7	−50.8
Clay loam	5.00	10.00	20.00	−77.4	−68.2	−63.0	−56.3
Silty clay loam	5.00	10.00	20.00	−68.0	−60.4	−53.9	−57.8
Sandy clay	5.00	10.00	15.00	−59.2	−57.1	−61.6	−39.7
Silty clay	5.00	10.00	20.00	−77.8	−77.8	−74.6	−61.7
Clay	5.00	20.00	40.00	−64.3	−68.7	−72.3	−51.2

[a] RMSE is calculated in terms of wetting front location z_j for vertical infiltration and Boltzmann variable ϕ_j for horizontal infiltration.
[b] The percent change in RMSE is calculated as 100 × (TO Diffusion RMSE – TO RMSE)/(TO RMSE). A negative value indicates that the RMSE is reduced by using TO Diffusion.

effects on the infiltration rate and cumulative infiltration amount are small. Due to the fact that the TO Diffusion method mostly redistributes portion of the infiltrated water in spreading the water content profiles due to diffusive effects, it is not surprising that the impact of this redistribution process does not significantly affect the total infiltration amount, which once again signifies the philosophy of separating diffusive and advection effects in redistributing the water amount due to diffusive effects.

As a final note of potential future studies, the idea of discretizing not in space but in the water-content domain provides the opportunity to mathematically describe macroporous flows. The macropores in the soil domain can be treated as a moisture bin embedded in the matrix, dominated by gravity and pressure-driven flow physics. The exchange between the matrix and macropores can be mathematically treated similarly to the water redistribution among bins. We are currently working on extending the ideas to flows involving macropores.

5. Summary and conclusions

In this study, we have developed a new method (TO Diffusion method) to better represent diffusive effects to the finite water-content method (TO method) by Ogden et al. (2015c) and Talbot and Ogden (2008). The TO Diffusion method retains the philosophy of the original TO method to discretize the water content domain into numerous bins, but treats advection and diffusion separately and explicitly considers the diffusive effects on a bin-by-bin basis. The method was evaluated by comparing with the solutions of the Richards equation for both horizontal and vertical infiltrations under saturated inlet surface boundary conditions, which represent the two extreme ends of the diffusion and advection scenarios.

The most fundamental consideration (assumption) of the approach is to separately deal with diffusive and advective effects for each water content bin at each time step. The advection has been already taken into account in the original finite water-content method. The focus of this study is to better capture the diffusive effects. The application of developed solution is straightforward only involving algebraic calculations at each time step.

The TO Diffusion method can mainly improve water content profiles. There is no significant difference for the total infiltration rate and cumulative infiltration compared to the TO method. Overall, the TO Diffusion method reduces the RMSE of water content profiles by 39% when both vertical and horizontal infiltrations are considered, which means that the proposed TO Diffusion approach can better simulate water content profiles than the TO method. The method under-predicts the diffusive effects in horizontal infiltration, but over-predicts them in vertical infiltration for coarse textural soils. Although it is a simple way to separately deal with advection and diffusion, the TO Diffusion method can account for the coupling effects of advection and diffusion reasonably well.

Acknowledgements

This work was partly funded by the U.S. National Science Foundation (NSF), EPSCoR program through cooperative agreement 1135483 Collaborative Research: CI-WATER, Cyberinfrastructure to Advance High Performance Water Resource Modeling, NSF EAR-1360384 WSC-Category 2 Collaborative Research: Planning and Land Management in a Tropical Ecosystem: Complexities of Land-use and Hydrology Coupling in the Panama Canal Watershed, and the Smithsonian Tropical Research Institute, the Wyoming Center for Environmental Hydrology and Geophysics (WyCEHG) EPSCoR Research Infrastructure Improvement (RII) Track-1 project, funded by NSF, and the Faculty Grant-In-Aid program at the University of Wyoming (1100-21266-2015).

Appendix A

1. The integral in Eq. (7) can be expressed in two parts as follows,

$$W = \left(\frac{1}{2}\right)(\theta_0 - \theta_{\text{ini}})(I_1 + I_2) \tag{A1}$$

where

$$I_1 = \int_{Ut}^{\infty} \operatorname{erfc}\left[\frac{z-Ut}{2\sqrt{Dt}}\right] dz = \int_0^{\infty} \operatorname{erfc}\left[\frac{y}{2\sqrt{Dt}}\right] dy = \frac{2\sqrt{Dt}}{\sqrt{\pi}} \tag{A2}$$

$$I_2 = \int_{Ut}^{\infty} \exp\left(\frac{Uz}{D}\right) \operatorname{erfc}\left[\frac{z+Ut}{2\sqrt{Dt}}\right] dz = \exp\left(-\frac{U^2 t}{D}\right) \int_{2Ut}^{\infty} \exp\left(\frac{Uy}{D}\right) \operatorname{erfc}\left[\frac{y}{2\sqrt{Dt}}\right] dy \tag{A3}$$

Since,

$$\int \exp\left(\frac{Uy}{D}\right) \operatorname{erfc}\left[\frac{y}{2\sqrt{Dt}}\right] dy = \frac{D}{U}\left\{\exp\left(\frac{Uy}{D}\right) \operatorname{erfc}\left[\frac{y}{2\sqrt{Dt}}\right] + \exp\left(\frac{U^2 t}{D}\right) \operatorname{erf}\left(\frac{y}{2\sqrt{Dt}} - U\sqrt{\frac{t}{D}}\right)\right\},$$

we have,

$$\begin{aligned}\int_{2Ut}^{\infty}\exp\left(\frac{Uy}{D}\right)\mathrm{erfc}\left[\frac{y}{2\sqrt{Dt}}\right]dy &= \frac{D}{U}\left\{\exp\left(\frac{U\infty}{D}\right)\mathrm{erfc}\left[\frac{\infty}{2\sqrt{Dt}}\right]\right.\\ &\left.+\exp\left(\frac{U^2t}{D}\right)\mathrm{erf}\left(\frac{\infty}{2\sqrt{Dt}}-U\sqrt{\frac{t}{D}}\right)\right\}\\ &-\frac{D}{U}\left\{\exp\left(\frac{U2Ut}{D}\right)\mathrm{erfc}\left[\frac{2Ut}{2\sqrt{Dt}}\right]\right.\\ &\left.+\exp\left(\frac{U^2t}{D}\right)\mathrm{erf}\left(\frac{2Ut}{2\sqrt{Dt}}-U\sqrt{\frac{t}{D}}\right)\right\}\\ &=\frac{D}{U}\left\{0+\exp\left(\frac{U^2t}{D}\right)\right\}\\ &-\frac{D}{U}\left\{\exp\left(\frac{2U^2t}{D}\right)\mathrm{erfc}\left(U\sqrt{\frac{t}{D}}\right)\right.\\ &\left.+\exp\left(\frac{U^2t}{D}\right)\mathrm{erf}(0)\right\}\\ &=\frac{D}{U}\exp\left(\frac{U^2t}{D}\right)\left\{1\right.\\ &\left.-\exp\left(\frac{U^2t}{D}\right)\mathrm{erfc}\left(U\sqrt{\frac{t}{D}}\right)\right\}\end{aligned}\tag{A4}$$

Therefore,

$$\begin{aligned}I_2 &= \exp\left(-\frac{U^2t}{D}\right)\int_{2Ut}^{\infty}\exp\left(\frac{Uy}{D}\right)\mathrm{erfc}\left[\frac{y}{2\sqrt{Dt}}\right]dy\\ &=\frac{D}{U}\left[1-\exp\left(\frac{U^2t}{D}\right)\mathrm{erfc}\left(U\sqrt{\frac{t}{D}}\right)\right]\\ &=\frac{D}{U}[1-\exp(\xi^2)\mathrm{erfc}(\xi)]\end{aligned}\tag{A5}$$

where

$$\xi = U\sqrt{\frac{t}{D}}\tag{A6}$$

We can then express the diffusive amount at any time t as,

$$\begin{aligned}W &= \left(\frac{1}{2}\right)(\theta_0-\theta_{\mathrm{ini}})(I_1+I_2)\\ &=\left(\frac{1}{2}\right)(\theta_0-\theta_{\mathrm{ini}})\left\{\frac{2\sqrt{Dt}}{\sqrt{\pi}}+\frac{D}{U}[1-\exp(\xi^2)\mathrm{erfc}(\xi)]\right\}\\ &=\left(\frac{\sqrt{Dt}}{2}\right)(\theta_0-\theta_{ini})\left\{\frac{2}{\sqrt{\pi}}+\frac{\sqrt{Dt}}{Ut}[1-\exp(\xi^2)\mathrm{erfc}(\xi)]\right\}\\ &=\left(\sqrt{\frac{Dt}{\pi}}\right)(\theta_0-\theta_{\mathrm{ini}})\left\{1+\frac{\sqrt{\pi}[1-\exp(\xi^2)\mathrm{erfc}(\xi)]}{2\xi}\right\}\end{aligned}\tag{8}$$

2. Under the condition when $\xi_t=\frac{Ut}{\sqrt{Dt}}\to 0$, we have

$$\begin{aligned}\lim_{\xi_t\to 0}\frac{1-\exp(\xi_t^2)\mathrm{erfc}(\xi_t)}{\xi_t} &= \lim_{\xi_t\to 0}\left\{-\left[\exp(\xi_t^2)\left(-\frac{2}{\sqrt{\pi}}\exp(-\xi_t^2)\right)\right.\right.\\ &\left.\left.+2\xi_t\exp(\xi_t^2)\mathrm{erfc}(\xi_t)\right]\right\}\\ &=\lim_{\xi_t\to 0}\left\{-\left[\left(-\frac{2}{\sqrt{\pi}}\right)+0\right]\right\}=\frac{2}{\sqrt{\pi}}\end{aligned}\tag{A7}$$

which indicates,

$$\lim_{\xi_t\to 0}\frac{\sqrt{\pi}}{2}\cdot\frac{1-\exp(\xi_t^2)\mathrm{erfc}(\xi_t)}{\xi_t}=1\tag{A8}$$

Therefore, from Eqs. (10) and (11) we have,

$$\lim_{\xi_t\to 0}W|_{t_i}=2\left(\sqrt{\frac{Dt_i}{\pi}}\right)(\theta_0-\theta_{\mathrm{ini}})\tag{A9}$$

$$\lim_{\xi_t\to 0}W|_{t_{i-1}}=2\left(\sqrt{\frac{Dt_{i-1}}{\pi}}\right)(\theta_0-\theta_{\mathrm{ini}})\tag{A10}$$

$$\lim_{\xi_t\to 0}\Delta W=2\sqrt{\frac{D}{\pi}}(\sqrt{t_i}-\sqrt{t_{i-1}})(\theta_0-\theta_{\mathrm{ini}})\tag{A11}$$

On the other hand, when $\xi_t=U\sqrt{\frac{t}{D}}$ is large such as in a case of strongly advective vertical infiltration, we have

$$\begin{aligned}\lim_{\xi_t\to\infty}\exp(\xi_t^2)\mathrm{erfc}(\xi_t) &= \lim_{\xi_t\to\infty}\frac{\mathrm{erfc}(\xi_t)}{\exp(-\xi_t^2)}=\lim_{\xi_t\to\infty}\frac{-\frac{2}{\sqrt{\pi}}\exp(-\xi_t^2)}{-2\xi_t\exp(-\xi_t^2)}\\ &=\lim_{\xi_t\to\infty}\frac{1}{\sqrt{\pi}\xi_t}=0\end{aligned}\tag{A12}$$

Therefore,

$$\lim_{\xi_t\to\infty}\frac{1-\exp(\xi_t^2)\mathrm{erfc}(\xi_t)}{\xi_t}=0\tag{A13}$$

$$\begin{aligned}\lim_{\xi_t\to\infty}W &= \left(\sqrt{\frac{Dt}{\pi}}\right)(\theta_0-\theta_{\mathrm{ini}})\left\{1+\frac{\sqrt{\pi}[1-\exp(\xi^2)\mathrm{erfc}(\xi)]}{2\xi}\right\}\\ &=\left(\sqrt{\frac{Dt}{\pi}}\right)(\theta_0-\theta_{\mathrm{ini}})\end{aligned}\tag{A14}$$

$$\lim_{\xi_t\to\infty}\Delta W=\sqrt{\frac{D}{\pi}}(\sqrt{t_i}-\sqrt{t_{i-1}})(\theta_0-\theta_{\mathrm{ini}})\tag{A15}$$

When flow scenario switches from $U\to 0$ to $U\to\infty$, the ratio of diffusive effects is,

$$\frac{\lim_{\xi_t\to 0}\Delta W}{\lim_{\xi_t\to\infty}\Delta W}=2\tag{25}$$

References

Brooks, R.H., Corey, A.T., 1964. Hydraulic Properties of Porous Media. Hydrol. Pap. 3, Colorado State University, Fort Collins, Colorado, U.S.

Caviedes-Voullieme, D., Garcia-Navarro, P., Murillo, J., 2013. Verification, conservation, stability and efficiency of a finite volume method for the 1D Richards equation. J. Hydrol. 480, 69–84. http://dx.doi.org/10.1016/j.jhydrol.2012.12.008.

Celia, M.A., Bouloutas, E.T., Zarba, R.L., 1990. A general mass-conservative numerical solution for the unsaturated flow equation. Water Resour. Res. 26, 1483–1496.

Green, W.H., Ampt, G.A., 1911. Studies of soil physics, part I – the flow of air and water through soils. J. Agric. Sci. 4, 1–24.

Lai, W., Ogden, F.L., 2015. A mass-conservative finite volume predictor–corrector solution of the 1D Richards' equation. J. Hydrol. 523, 119–127. http://dx.doi.org/10.1016/j.jhydrol.2015.01.053.

Liang, W., Uchida, T., 2014. Effects of topography and soil depth on saturated-zone dynamics in steep hillslopes explored using the three-dimensional Richards' equation. J. Hydrol. 510, 124–136. http://dx.doi.org/10.1016/j.jhydrol.2013.12.029.

Menziani, M., Pugnaghi, S., Vincenzi, S., 2007. Analytical solutions of the linearized Richards equation for discrete arbitrary initial and boundary conditions. J. Hydrol. 332, 214–225. http://dx.doi.org/10.1016/j.jhydrol.2006.06.030.

Miller, C.T., Williams, G.W., Kelly, C.T., Tocci, M.D., 1998. Robust solution of Richards equation for nonuniform porous media. Water Resour. Res. 34, 2599–2610.

Morel-Seytoux, H.J., Meyer, P.D., Nachabe, M., Touma, J., Van Genuchten, M.Th., Lenhard, R.J., 1996. Parameter equivalence for the Brooks – Corey and van Genuchten soil characteristics: preserving the effective capillary drive. Water Resour. Res. 32 (5), 1251–1258.

Ogden, F.L., Lai, W., Steinke, R.C. 2015. ADHydro: Quasi-3D high performance hydrological model. In: Proceedings of SEDHYD 2015, 10th Interagency Sedimentation Conference, 5th Federal Interagency Hydrologic Modeling

Conference April 19–23, Reno, Nevada, USA. pp. 342–350 <http://acwi.gov/sos/pubs/3rdJFIC/index.html> (Accessed 18 December 2015).
Ogden, F.L., Lai, W., Steinke, R.C., Zhu, J., 2015b. Validation of finite water-content vadose zone dynamics method using column experiments with a moving water table and applied surface flux. Water Resour. Res. 51, 3108–3125. http://dx.doi.org/10.1002/2014WR016454.
Ogden, F.L., Lai, W., Steinke, R.C., Zhu, J., Talbot, C.A., Wilson, J.L., 2015c. A new general 1-D vadose zone flow solution method. Water Resour. Res. 51, 4282–4300. http://dx.doi.org/10.1002/2015WR017126.
Ogata, A., Banks, R.B. 1961. A solution of the differential equation of longitudinal equation in porous media. U.S. Geological Survey Professional Paper 411-A.
Rawls, W.J., Brakensiek, D.L., Saxton, K.E., 1982. Estimation of soil water properties. Trans. ASAE 25 (5), 1316–1330.
Rawls, W.J., Brakensiek, D.L., Miller, N., 1983. Green –Ampt infiltration parameters from soils data. J. Hydraulic Eng., ASCE 109 (1), 62–70.
Richards, L.A., 1931. Capillary conduction of liquids in porous mediums. Physics 1 (5), 318–333.
Simunek, J., Sejna, M., Saito, H., Sakai, M., van Genuchten, M.T., 2009. The HYDRUS-1D Software Package for Simulating the One-dimensional Movement of Water, Heat, and Multiple Solutes in Variably-saturated Media. University of California Riverside, Riverside, CA.
Talbot, C.A., Ogden, F.L., 2008. A method for computing infiltration and redistribution in a discretized moisture content domain. Water Resour. Res. 44 (8). http://dx.doi.org/10.1029/2008WR006815.
van Dam, J.C., Feddes, R.A., 2000. Numerical simulation of infiltration, evaporation and shallow groundwater levels with the Richards equation. J. Hydrol. 233, 72–85.
van Genuchten, M.Th., 1980. A closed-form equation for predicting the hydraulic conductivity of unsaturated soils. Soil Sci. Soc. Am. J. 44, 892–898.
Vogel, T., van Genuchten, M.Th., Cislerova, M., 2001. Effect of the shape of the soil hydraulic functions near saturation on variably saturated flow predictions. Adv. Water Resour. 24 (2), 133–144.